

MOL 37564

Pharmacological characterization of a novel nonpeptide antagonist for formyl peptide receptor-like 1

Caihong Zhou, Song Zhang, Masakatsu Nanamori, Yueyun Zhang, Qing Liu, Na Li, Meiling Sun, Jun Tian, Patrick P. Ye, Ni Cheng, Richard D. Ye, and Ming-Wei Wang

The National Center for Drug Screening, Shanghai Institute of Materia Medica (C.Z., Y.Z., Q.L., N.L., M.S., M.-W.W.) and the Graduate School (S.Z.), Chinese Academy of Sciences, Shanghai , China; Department of Pharmacology, College of Medicine, University of Illinois, Chicago, Illinois (M.N., J.T., P.P.Y., N.C., R.D.Y)

MOL 37564

Running title: Quinazolinone antagonist for FPRL1

Address correspondence to: Ming-Wei Wang, the National Center for Drug Screening, 189

Guo Shou Jing Road, Shanghai 201203, China. E-mail: mwwang@mail.shcnc.ac.cn

Number of text pages: 24

Number of tables: 1

Number of figures: 10

Number of References: 20

Number of words in Abstract: 171

Number of words in Introduction: 495

Number of words in Discussion: 1125

Abbreviations

FPRL1, formyl peptide receptor-like 1; SAR, structure-activity relationships; WKYMVm, Trp-Lys-Tyr-Met-Val-D-Met-NH₂; WRW⁴, Trp-Arg-Trp-Trp-Trp-Trp-NH₂; fMLF, N-formyl-Met-Leu-Phe; DMEM, Dulbecco's modified Eagle's medium; FBS, fetal bovine serum; HBSS, Hanks's balanced saline solution; BSA, bovine serum albumin; PBS, phosphate-buffered saline; NF- κ B, nuclear factor- κ B; ERK, extracellular signal-regulated kinase; DMSO, dimethyl sulfoxide; Fluo-4/AM, 1-[2-Amino-5-(2,7-difluoro-6-hydroxy-3-oxo-9-xanthenyl)phenoxy]-2-(2-amino-5-methylphenoxy)ethane-N,N,N',N'-tetraacetic acid, pentaacetoxymethyl ester; AA, arachidonic acid.

MOL 37564

Abstract

A series of quinazolinone derivatives were synthesized based on a hit compound identified from a high-throughput screening (HTS) campaign targeting the human formyl peptide receptor-like 1 (FPRL1). Based on structure-activity relationship (SAR) analysis, we found that substitution on the *para* position of the 2-phenyl group of the quinazolinone backbone could alter the pharmacological properties of the compound. The methoxyl substitution produced an agonist Quin-C1 (C1), whereas a hydroxyl substitution resulted in a pure antagonist, Quin-C7 (C7). Several partial agonists were derived from other substitutions on the *para* position. C7 partially displaced [125 I]WKYMVm binding to FPRL1 but not [3 H]fMLF to FPR. In functional assays using FPRL1-expressing RBL-2H3 cells, C7 inhibited calcium mobilization and chemotaxis induced by WKYMVm and C1, as well as degranulation elicited by C1. C7 also suppressed C1-induced ERK phosphorylation and reduced arachidonic acid-induced ear edema in mice. This study represents the first characterization of a nonpeptidic antagonist for FPRL1 and suggests the prospect of using low molecular weight compounds as modulators of chemoattractant receptors *in vitro* and *in vivo*.

MOL 37564

Introduction

The human formyl peptide receptor (FPR) family of chemoattractant receptors consists of FPR, formyl peptide receptor-like 1 (FPRL1), and FPRL2. These receptors are expressed primarily in neutrophils and monocytes, and exert important functions in inflammation and immunity (Le et al., 2002). The FPRL1 gene was initially cloned in 1992 for its homology with FPR cDNA (Bao et al., 1992; Murphy et al., 1992; Ye et al., 1992). The prototype of chemotactic peptide N-formyl-Met-Leu-Phe (fMLF), an agonist for FPR, can also activate FPRL1 with a reduced affinity (Quehenberger et al., 1993). Stimulation of FPRL1 elicits a cascade of host defense reactions against pathogens, including chemotaxis, superoxide generation, and exocytosis in human neutrophils. In addition, it was also reported that FPRL1 attenuates HIV-1 infection by desensitizing and down-regulating the chemokine receptors CCR5 and CXCR4, which serve as major co-receptors for HIV-1, on monocyte surfaces (Li et al., 2001). A recent study showed that the expression of FPRL1 in mouse C26 cells markedly reduced tumorigenicity in syngeneic mice and resulted in high levels of humoral immune response to both FPRL1-containing and wild type C26 cells (Hu et al., 2005). The data indicate that FPRL1 also plays a key role in specific anti-tumor response. The expression of FPRL1 in activated microglial cells and its function as a receptor for A β (1-42), a 42-amino acid form of the β amyloid peptide, suggest that FPRL1 is closely related to neurodegenerative disorders (Hu et al., 2005). Investigation in ligand binding, signal transduction and functional properties of FPRL1 is expected to facilitate the understanding of this receptor as a new therapeutic target.

Among the FPR family of receptors, FPRL1 has the broadest spectrum of ligands (Migeotte et al., 2006). Except one lipid (lipoxin A4), all identified FPRL1 ligands are small peptides and include host-derived agonist LL-37, natural or synthetic peptides (humanin, MMK-1 and WKYMVm), and peptides derived from HIV-1 envelope proteins (De et al., 2000; Le et al., 1999). These pharmacological properties of FPRL1 imply that it is a potential target for therapeutic intervention. However, identification of antagonists for this receptor has met with difficulties. Recently, a new peptide (WRWWWW; WRW⁴) was identified as an antagonist for FPRL1 by screening a hexapeptide library (Bae et al., 2003). Because of inherent limitations of peptides as therapeutic agents, it is desirable to develop synthetic,

MOL 37564

nonpeptidic ligands for receptors. Not long ago, we initiated a high-throughput screening (HTS) campaign to identify FPRL1 ligands from a synthetic compound library. Following vigorous screening and structure modification, a substituted quinazolinone compound (Quin-C1;

4-butoxy-N-[2-(4-methoxy-phenyl)-4-oxo-1,4-dihydro-2H-quinazolin-3-yl]-benzamide) was discovered. This compound (C1) displayed selective agonistic effects on FPRL1 (Nanamori et al., 2004). As an ongoing effort to study the structure-activity relationship (SAR) of the original compound, we designed, synthesized and characterized a series of substituted quinazolinone derivatives as modulating agents for FPRL1. Our results indicate that a hydroxyl substitution on the *para* position of the 2-phenyl group of the quinazolinone backbone resulted in a pure antagonist, Quin-C7 (C7), which displayed inhibitory effects on FPRL1.

MOL 37564

Materials and Methods

Materials. WKYMVm was synthesized at GL Biochem (Shanghai) Ltd. (Shanghai, China). WRW⁴ and MMK-1 were made at HD Biosciences Co. (Shanghai, China). [¹²⁵I]-WKYMVm (Bolton-Hunter labeled), [³H]fMLF and FlashBlueTM GPCR scintillating beads were obtained from PerkinElmer (Boston, MA). Steady-GloTM Luciferase Assay Solutions were purchased from Promega Corporation (Madison, WI). Fluo-4/AM was the product of Molecular Probes (Eugene, OR). DMEM culture medium and trypsin were bought from Life Technologies (Grand Island, NY). Fetal bovine serum (FBS) was purchased from Hyclone Co. (St. Louis, MO). The anti-ERK1/2 and anti-phospho-ERK antibodies were procured from Cell Signaling Technologies (Beverly, MA). Other reagents were supplied by Sigma Chemical Co. (St. Louis, MO).

Cell Culture. The human cervical carcinoma cell line HeLa was transfected with pNF-κB-Luc reporter plasmid that contains 5 copies of NF-κB binding sequence (Stratagene, La Jolla, CA) and a human FPRL1 cDNA expression vector in pSFFV.neo vector as reported (Nanamori et al., 2004; Tian et al., 2005). The transfected cells were maintained in Dulbecco's modified Eagle's medium (DMEM) supplemented with 10% FBS. Rat basophilic leukemia cell line RBL-2H3 expressing either the human FPRL1 or human FPR was described previously and maintained in DMEM supplemented with 20% FBS (He et al., 2000).

Compound Synthesis. The quinazolinone series compounds were synthesized according to the method described previously (Mayer et al., 1997) and the synthetic route is shown in Figure 1. Anthranilic acid derivative **5** was obtained subsequently via reduction of compound **4** with zinc and acetic acid in CH₂Cl₂. Moderate to high yield was achieved through refluxing compound **5** with different substituted benzaldehydes in a mixed solvent (CH₂Cl₂/DMA catalyzed by acetic acid), using molecular sieve as dehydrate reagent.

Ligand Binding Assay. Ligand binding assay was performed as previously described (Yan et al., 2006). RBL-FPRL1 cells (~10⁹) were harvested and washed twice with PBS. Cell membrane was prepared with BioNeb Cell Disruption System (Glas-Col, Terre Haute, Indiana). Various concentrations of compounds were incubated together with RBL-FPRL1 cell membrane preparation, 0.16 nM [¹²⁵I]WKYMVm (PerkinElmer, K_d = 0.32 nM) and

MOL 37564

FlashBlue™ GPCR beads (100 µg/well) to give a final volume of 0.1 ml. The plates were incubated at 4°C for 12 h and centrifuged for 3 min at 2500 × g before counting on a MicroBeta scintillation counter (PerkinElmer). To test the binding affinity for FPR, RBL-FPR cells (1×10^5) were seeded onto 24-well plates and incubated for 48 h. After being washed twice with blocking buffer (RPMI1640 supplemented with 25 mM HEPES and 0.1% BSA, pH7.5), cells were incubated with blocking buffer for 2 h, then sequentially with 30 nM [³H]fMLF and different concentrations of C7 or unlabeled fMLF in binding buffer (PBS with 10% BSA) for another 2 h. Radioactivity was measured as above.

Reporter Assay. HeLa cells expressing NF-κB-Luc/FPRL1 (HeLa-κB-FPRL1) were seeded onto 96-well plates at a density of 1.5×10^4 cells per well. After cells became adherent, they were serum-starved in DMEM for 16 h prior to screening assay. Different concentrations of compounds were added to the cells for 5 h, the expressed luciferase activity was determined in an EnVision 2101 multilabel reader (PerkinElmer) using the Steady-Glo™ Luciferase Assay solutions.

Calcium Mobilization Assay. Calcium mobilization assay was performed as previously described (Yan et al., 2006). Briefly, RBL-FPRL1 cells were detached and collected by centrifugation, loaded with 5 µM Fluo-4/AM (Molecular Probes) in Hank's balanced salt solution (HBSS) supplemented with 2.5 mM probenecid for 45 min, and then washed twice with HBSS. Cell suspensions were adjusted to a density of 5×10^6 cells/ml and seeded onto 96-well plates (100 µl per well). Cells were reattached by centrifugation and then analyzed for calcium mobilization using FlexStation™ (Molecular Devices, Sunnyvale, CA) with excitation wavelength at 485 nm and emission wavelength at 525 nm. For antagonist mode, cells were incubated with or without test compounds for 15 min before the addition of WKYMVm (2 nM) or C1 (5 µM). For detailed characterization of RBL-FPRL1 cells, calcium mobilization assays were conducted on a spectrofluorometer (Photon Technology Inc, Lawrenceville, NJ), using as indicator Indo-1 and procedures described previously (Nanamori et al., 2004)

Chemotaxis. WKYMVm and C1-induced migration of cells was assessed in a 48-well micro-chemotaxis chamber (Neuro Probe, Cabin John, MA) as previously described (Nanamori et al., 2004). Briefly, WKYMVm (10 nM, 30 µl) or C1 (100 nM, 30 µl) were

MOL 37564

placed in the lower chamber, RBL-FPRL1 cells ($50\ \mu\text{l}$ at 1×10^6 cells/ml) were pre-incubated with or without test compounds for 15 min and then loaded in the upper chamber, which was separated from the lower chamber by a polycarbonate filter (pore size $8\ \mu\text{m}$). After incubation at 37°C for 4 h, the filter was removed, fixed and stained with Diff-Quick staining solutions (IMEB Inc., San Marcos, CA). Chemotaxis was quantified by counting migrated cells in five randomly chosen high power fields ($400\times$).

Phosphorylation of Mitogen-activated Protein Kinases. Activation of the p44/p42 MAP kinases (ERK1/2) was determined essentially as described previously (Nanamori et al., 2004). Briefly, cells were cultured in 6-well plates and serum starved overnight prior to agonist stimulation. Some samples were pretreated with the antagonist (C7) for 15 min prior to agonist (C1) stimulation for 5 min. The reaction was terminated by adding $300\ \mu\text{l}$ ice-cold SDS-PAGE loading buffer [15% (v/v) glycerol, 125 mM Tris-Cl, pH 6.8, 5 mM EDTA, 2% (w/v) SDS, 0.1% bromophenol blue and 1% β -mercaptoethanol]. Samples were sonicated to disperse DNA contents. After boiling, samples were analyzed by SDS-PAGE and Western blot using anti-ERK1/2 and anti-phospho-ERK1/2 antibodies at 1:1000 dilution. HRP-conjugated anti-rabbit antibody (1:3000) was used as secondary antibody. The resulting immunocomplex was visualized by SuperSignal West Pico Chemiluminescence (Pierce, Rockford, IL).

Ear Edema Assay. Male BALB/c mice weighing 20-24 g (Shanghai SLAC Laboratory Animals Co., China) were used in the experiment. The animals were housed in an environmentally (25°C) and air humidity (60%) controlled room with a 12 h light-dark cycle, and kept on a standard laboratory diet and drinking water *ad libitum*. Mice were fasted for 18 h with free access to water and divided into groups of 4 or 7 animals. The study was conducted according to the procedures approved by the institutional animal care committee.

Inflammation was induced by arachidonic acid (AA) as described previously with minor modifications (Rao et al., 1993). Briefly, AA (0.25 mg in $20\ \mu\text{l}$ 5% DMSO and 95% acetone) was topical applied onto both surfaces of the right ear of each mouse. Left ear (control) received solvent treatment. C7, at various doses dissolved in 1% DMSO, 19% PEG400 and 80% normal saline, was administered i.p. ($200\ \mu\text{l}$) 0.5 h before AA application. Two control groups were used: one was treated with vehicle and the other received dexamethasone (1 mg).

MOL 37564

Inflammation was induced for 3 h following AA application and the animals were sacrificed by cervical dislocation. An 8 mm section from each ear was removed with a metal punch and weighted immediately. Ear edema was determined by subtracting the weight of the left ear from that of the right ear. The rate of edema (%) was calculated by dividing the weight difference between the left and right ear with the left ear weight and multiplied by 100.

MOL 37564

Results

Characterization of quinazolinone derivatives as FPRL1 ligands. In a previous study, we conducted an HTS of 15,760 synthetic and 400 natural compounds. Among these, 3 compounds were found to be potential FPRL1 agonists. Based on one hit compound, whose core structure is shown in Figure 2A, we developed the first nonpeptidic ligand Quin-C1 for FPRL1 (Nanamori et al., 2004). In order to search for FPRL1 antagonists, four series of quinazolinone derivatives (C, M, W and O) were synthesized (Figure 2A). Few compounds in the M, W and O series showed activity. The preliminary SAR analysis of C series compounds indicated that the substitution of the phenyl group at the 2-position of quinazolinone backbone might be a possible determinant for its functional property. Thus, more derivatives of C series were made (Figure 2B) in accordance with the method described previously (Mayer et al., 1997). Amino substituted compound (C11) was obtained by reduction of its corresponding nitro substituted compound (C10).

In order to determine the substituted position, four compounds were synthesized first. There was a methoxy group at the 4'-position in C1, and a 2',4'-disubstitution in C2 and C4. C6 contains no substitution in the aromatic ring. These modifications produced drastically different effects: among these compounds, C2, C4 and C6 lost agonist activity entirely in the calcium mobilization assay (Supplement Figure 1). However, C1 showed a stronger agonist activity than that of the hit compound (Table 1).

Next, compounds with different substitutions at the 4'-position were synthesized to study the impacts of the substituted groups. C1 (4'-methoxy), C5 (4'-methyl), and C10 (4'-nitro) exhibited strong agonist activity (Table 1). Substitutions with bulky groups, *e.g.*, *t*-butoxy (C9) or *n*-butoxy (C12), resulted in decreased or loss of bioactivity. Bioactivity also decreased when the nitro was changed to amino (C11) and lost when changed to N,N-dimethylamino group (C3). Of particular interest is the complete reversal of bioactivity when the methoxy group was substituted with a hydroxyl group (C7). This substitution resulted in an antagonist for FPRL1 (see below).

C7 inhibits WKYMVm stimulated calcium mobilization. Though C7 showed a higher binding affinity than C9, which exhibited bioactivity in reporter assay, no agonist activity was detected in both reporter and calcium mobilization assays (Table 1). Since the reporter assay

MOL 37564

involves the activation of several signaling pathways and is distal from the receptor, we conducted additional studies to study the proximal signaling events induced by the activated receptor. Further characterization was conducted with C7 and C12 in calcium mobilization assays. Calcium mobilization results from FPRL1-activated PLC β , which generates the second messengers diacyl glycerol and inositol 1,4,5-trisphosphate. The RBL-FPRL1 cell line, used in this and other functional studies described in this paper, was generated through stable expression of the human FPRL1 cDNA. RT-PCR analysis showed that it does not contain transcript for human FPR and FPRL2 (Figure 3A). In calcium mobilization assays (Figure 3B), the cell line responded strongly to WKYMVm (100 nM); it responded to C1 at a higher concentration (100 μ M), but was sensitive to the FPRL1-selective agonist MMK1 (100 nM). However, RBL-FPRL1 only weakly responded to fMLF (100 nM), a high-affinity agonist for FPR and low-affinity agonist for FPRL1. F2L, an agonist for FPRL2, did not induce calcium mobilization (data not shown). These results confirmed that the observed calcium mobilization was mediated by FPRL1 but not the structurally related FPR or FPRL2. As shown in Figure 4, C7 antagonized WKYMVm stimulated calcium mobilization in a dose-dependant manner, while C12 inhibited WKYMVm stimulated calcium mobilization no more than 20% at concentrations up to 100 μ M.

C7 suppresses chemotaxis in C1 and WKYMVm stimulated RBL-FPRL1 cells. In chemotaxis assay, C7 inhibited C1-induced cell migration in a dose-dependent manner (Figure 5). Given the structural similarity between these two compounds, the antagonistic effect was expected. Interestingly, C7 also suppressed chemotaxis induced by WKYMVm, a highly potent FPRL1 agonist with no structural resemblance to C7. Our earlier study suggested a partial overlap between C1 and WKYMVm in FPRL1 binding (Nanamori et al., 2004). The data shown in Figure 5 could be partially explained with the homologous structures of C7 and C1. Our results also indicate that C7 could reduce WKYMVm-stimulated degranulation by up to 57% (data not shown) as well as C1-induced degranulation in a dose-dependent manner (Supplement Figure 2) in RBL-FPRL1 cells.

C7 and its analogues compete with WKYMVm for binding to RBL-FPRL1 cells. In order to study the binding properties of C7 and other C series compounds to FPRL1, competitive binding assays using [125 I]WKYMVm were performed with membranes prepared

MOL 37564

from RBL-FPRL1 cells. C7 and selected analogues competed effectively for binding to RBL-FPRL1 (Figure 6). Among the analogues studied, C1 and C5 are more potent than C7, exhibiting IC_{50} values of 92 ± 1 and 174 ± 61 nM, respectively. C7 could not completely displace [125 I]WKYMVm binding to FPRL1 at 100 μ M, the highest concentration used in the assay because of limited solubility of the compound. The IC_{50} of 6653 ± 859 nM (Table 1) was derived from maximal, but not complete, displacement of the radioligand. Although C7 is less potent than C1 in the competitive binding assay, it specifically interacts with FPRL1 but not FPR. In binding assays using FPR-transfected RBL cells, C7 at concentrations up to 100 μ M could not effectively compete with [3 H]fMLF for binding to the RBL-FPR cells (Figure 7).

C7 inhibits agonist-induced ERK phosphorylation. FPRL1-mediated activation of the MAP kinases, ERK1 and ERK2, was determined in C1-stimulated RBL-FPRL1 cells, based on activation-associated phosphorylation (Payne et al., 1991). Maximal activation was observed at ~5 min after agonist stimulation. When the cells were pretreated with C7, the agonist-induced phosphorylation of ERK1 and ERK2 was reduced (Figure 8). The inhibitory effect of C7 was evident at 3 μ M and above. At 100 μ M, C7 reduced phosphorylated ERK to its base level.

Comparing C7 with WRW⁴ for their antagonistic activities. To date, WRW⁴ is the only characterized peptide with selectivity for FPRL1 (Bae et al., 2004). The antagonistic effect of C7 was compared to that of WRW⁴ in calcium mobilization assay. WKYMVm-induced calcium mobilization in RBL-FPRL1 cells was dose-dependently inhibited by C7 (Figure 9A). Likewise, WRW⁴ displayed inhibitory effect in the calcium mobilization assay (Figure 9B). An analysis of the results demonstrated that C7 had comparable antagonist efficacy (90.6%) to WRW⁴, though its potency was not as good as WRW⁴. When C1 was used as agonist, the efficacy of C7 in the suppression of calcium release was similar to that of WRW⁴ (65.9% vs. 59.6%; Figures 9C and 9D).

C7 inhibits arachidonic acid-induced ear edema. The *in vivo* effect of C7 was determined in an ear edema model (Rao et al., 1993). BALB/c mice were treated with arachidonic acid (AA, right ears) or solvent (left ears). In testing groups, different concentrations of C7 were given i.p. to mice 0.5 h before AA application. A positive control group was included in which mice received dexamethasone instead of C7. Three hours later, animals were sacrificed

MOL 37564

and ear edema was determined as described in *Materials and methods*. As shown in Figure 10, C7 dose-dependently inhibited AA-induced ear edema. At concentrations of 1 mg and 5 mg, the inhibitory effects of C7 approached to that of dexamethasone (1 mg).

Discussion

We previously reported the identification of Quin-C1 (C1), the first synthetic, nonpeptidic agonist for FPRL1 identified through an HTS campaign (Nanamori et al., 2004). Quin-C1 is one of the quinazolinone derivatives prepared from a core structure identified from 16,160 compounds. A preliminary SAR study suggests that substitutions at the 4'-position of the 2-phenyl group of quinazolinone backbone play a key role for the bioactivity of the compounds, ranging from full agonists to full antagonists. These results indicate that small substitution groups at the 4'-position can exhibit modulatory effects. In this study, we describe the functional characterization of Quin-C7 (C7), which contains a hydroxyl group at the 4'-position and displays antagonistic effects in a variety of functional assays. In competitive binding assays, C7 showed binding affinity for FPRL1 below that of C1, C5 and C10, but higher than the binding affinities of C9, C11 and C12. This binding property is highly selective for FPRL1 as it did not compete the interaction between FPR and [³H]fMLF (Figure 7). It is notable that C7 was unable to completely displace [¹²⁵I]WKYMVm in competitive binding assays. Due to limitation of its solubility, C7 could not be used for more than 100 μ M in our assays. The binding data suggest that C7 is a partial antagonist for WKYMVm binding to FPRL1. As discussed below, WKYMVm and C7 may occupy partially overlapping binding sites on FPRL1 because of the difference in their structures. The fact that C7 was more effective in the inhibition of C1-induced than WKYMVm-induced responses (e.g., Figures 8 and 9) clearly reflects the structural similarities between C7 and C1. As shown in Figure 4, the inhibitory effect of C7 is specific for FPRL1 and not caused by cytotoxicity, because C12, a compound of the same structural group, was neither toxic nor bioactive when tested in the same system. Moreover, the RBL-FPRL1 cell line used in this study was an engineered cell line that expresses human FPRL1, but not human FPR or FPRL2 (Figure 3A). The selectivity of the cell line was confirmed in calcium mobilization assays, which displayed pharmacological properties of FPRL1 with functional responses to

MOL 37564

MMK1 and WKYMVm, but only weakly to fMLF (Figure 3B). Together, our data support the conclusion that C7 is a selective antagonist for FPRL1. Our attempt to generate a RBL cell line expressing human FPRL2 is not successful, probably due to the reported tendency of this receptor to express intracellularly (Migeotte et al., 2006). Therefore, the possibility that C7 acts on FPRL2 cannot be ruled out at this time.

The binding pockets of FPRL1 for its ligands have not been fully characterized. Based on the broad spectrum of ligand specificity, it is predicted that multiple binding sites exist in FPRL1 that allow its interaction with both peptides (e.g. A β ₁₋₄₂, MMK-1, SAA) and a lipid (lipoxin A₄). Our previous characterization revealed a partial interference between WKYMVm and C1 in binding assays (Nanamori et al., 2004). This may result from a partial overlap of the two binding sites, or an allosteric effect of one ligand that alters the binding of the other ligand. The C series compounds characterized in this work are derivatives of C1, and they likely share the same binding site with C1. The observation that C6, which contains no substitutions in the phenol ring and lost its bioactivity in the calcium mobilization assay, suggests that small substitution groups at the 4'-position are critical to the function of the compounds. However, disubstitutions such as those in C2 and C4, and bulky substitutions such as the ones in C3 and C12, produced no bioactivity in the calcium mobilization assay. This latter finding indicates that the binding pocket for the C series compounds is relatively small and cannot accommodate bulky groups or disubstitutions. The observation that these compounds bound poorly to FPRL1 supports the notion that a part of the binding pocket for the C series compounds provides very limited space.

Our preliminary SAR study also points to the importance for proper contact between the small substitution group at the 4'-position and the receptor's binding site. Such an interaction is crucial to the bioactivity of the compounds. Small substitution groups such as the methoxy, methyl and nitro groups are excellent for the agonistic activity, whereas a larger substitution group in C8 may be responsible for the reduced agonistic activity. Relative potency, both agonistic and antagonistic, may also require proper spacing between the contact sites such that compounds with an oxygen placed at the 4'-position of the phenol ring (C1 and C7) proves to be most efficacious. However, C9 and C12 are much less effective probably due to the larger size of the substitution groups.

MOL 37564

Chemoattractant receptors play a key role in the regulation of acute and chronic inflammation. In this study, we have shown that C7 effectively inhibited AA-induced ear edema, suggesting an *in vivo* effect of C7 in the suppression of inflammation. Several possibilities exist for this anti-inflammatory effect. First, C7 suppresses AA-induced ear edema through blockade of FPRL1, offsetting the pro-inflammatory effect of a FPRL1 agonist released by AA-treated cells. Supporting this possibility is our *in vitro* result indicating C7 as a selective antagonist for FPRL1. However, the exact agonist(s) produced by AA-stimulated cells are not known at present, as FPRL1 has particularly broad ligand selectivity and can respond to a variety of pro-inflammatory peptides (Migeotte et al., 2006). Secondly, C7 directly acts on FPRL1 as an anti-inflammatory ligand, in a manner similar to that of lipoxin A4. There are indeed similarities between the two agents as neither was able to perform like a typical agonist yet exhibited anti-inflammatory properties. The mechanism underlying the anti-inflammatory effect of lipoxin A4 has not been fully understood, but induction of SOCS-2 was shown to contribute to this effect (Machado et al., 2006). It would be interesting to determine whether C7 can also induce SOCS-2. Finally, it remains a possibility that C7 acts on a target molecule other than FPRL1. Although there is no direct evidence supporting the presence of another C7 target, the fact that C7 can reduce ear edema as effectively as dexamethasone is of interest and suggests the potential of developing an anti-inflammatory agent based on this lead compound.

As one of the primary chemoattractant receptors in neutrophils and monocytes, FPRL1 has a particularly broad ligand selectivity. However, progress has been slow in the identification of its antagonist. WRW⁴ was the first peptidic antagonist specifically targeting FPRL1, and its potency for maximal antagonism in the low μ M range is reasonably good. Though C7 was about 36- to 50-fold less potent than WRW⁴ in similar functional assays, it could attain comparable suppression efficacy in the calcium mobilization assay in RBL-FPRL1 cells. The current study suggests the possibility of improving its efficacy with further structural modifications.

MOL 37564

Acknowledgments

We thank Drs. Guangxing Wang and Dale E. Mais for valuable discussions, and Mr. Pangke Yan, Mr. Qinghai Tian, Ms. Xiaozhen Cheng, Ms. Huili Lu and Mr. Zhen Zhang for technical assistance.

MOL 37564

References

- Bae YS, Lee HY, Jo EJ, Kim JI, Kang HK, Ye RD, Kwak JY and Ryu SH (2004) Identification of peptides that antagonize formyl peptide receptor-like 1-mediated signaling. *J Immunol* **173**:607-614.
- Bae YS, Yi HJ, Lee HY, Jo EJ, Kim JI, Lee TG, Ye RD, Kwak JY and Ryu SH (2003) Differential activation of formyl peptide receptor-like 1 by peptide ligands. *J Immunol* **171**:6807-6813.
- Bao L, Gerard NP, Eddy RL, Shows TB and Gerard C (1992) Mapping genes for the human C5a receptor (C5AR), human FMLP receptor (FPR), and two FMLP receptor homologue orphan receptors (FPRH1, FPRH2) to chromosome 19. *Genomics* **13**:437-440.
- De Y, Chen Q, Schmidt AP, Anderson GM, Wang JM, Wooters J, Oppenheim JJ and Chertov O (2000) LL-37, the neutrophil granule- and epithelial cell-derived cathelicidin, utilizes formyl peptide receptor-like 1 (FPR1) as a receptor to chemoattract human peripheral blood neutrophils, monocytes, and T cells. *J Exp Med* **192**:1069-1074.
- He R, Tan L, Browning DD, Wang JM and Ye RD (2000) The synthetic peptide trp-lys-tyr-met-val-D-Met is a potent chemotactic agonist for mouse formyl peptide receptor. *J Immunol* **165**:4598-4605.
- Hu J, Li G, Tong Y, Li Y, Zhou G, He X, Xie P, Wang JM and Sun Q (2005) Transduction of the gene coding for a human G-protein coupled receptor FPR1 in mouse tumor cells increases host anti-tumor immunity. *Int Immunopharmacol* **5**:971-980.
- Le Y, Gong W, Li B, Dunlop NM, Shen W, Su SB, Ye RD and Wang JM (1999) Utilization of two seven-transmembrane, G protein-coupled receptors, formyl peptide receptor-like 1 and formyl peptide receptor, by the synthetic hexapeptide WKYMVm for human phagocyte activation. *J Immunol* **163**:6777-6784.
- Le Y, Murphy PM and Wang JM (2002) Formyl-peptide receptors revisited. *Trends Immunol* **23**:541-548.
- Li BQ, Wetzel MA, Mikovits JA, Henderson EE, Rogers TJ, Gong W, Le Y, Ruscetti FW and Wang JM (2001) The synthetic peptide WKYMVm attenuates the function of the chemokine receptors CCR5 and CXCR4 through activation of formyl peptide receptor-like 1. *Blood* **97**:2941-2947.
- Machado FS, Johndrow JE, Esper L, Dias A, Bafica A, Serhan CN and Aliberti J (2006) Anti-inflammatory actions of lipoxin A4 and aspirin-triggered lipoxin are SOCS-2 dependent. *Nat Med* **12**:330-334.
- Mayer JP, Lewis GS, Curtis MJ and Zhang J (1997) Solid phase synthesis of quinazolinones

MOL 37564

Tetrahedron Letters **38**:8445-8448.

Migeotte I, Communi D and Parmentier M (2006) Formyl peptide receptors: a promiscuous subfamily of G protein-coupled receptors controlling immune responses. *Cytokine Growth Factor Rev* **17**:501-519.

Murphy PM, Ozcelik T, Kenney RT, Tiffany HL, McDermott D and Francke U (1992) A structural homologue of the N-formyl peptide receptor. Characterization and chromosome mapping of a peptide chemoattractant receptor family. *J Biol Chem* **267**:7637-7643.

Nanamori M, Cheng X, Mei J, Sang H, Xuan Y, Zhou C, Wang MW and Ye RD (2004) A novel nonpeptide ligand for formyl peptide receptor-like 1. *Mol Pharmacol* **66**:1213-1222.

Payne DM, Rossomando AJ, Martino P, Erickson AK, Her JH, Shabanowitz J, Hunt DF, Weber MJ and Sturgill TW (1991) Identification of the regulatory phosphorylation sites in pp42/mitogen-activated protein kinase (MAP kinase). *EMBO J* **10**:885-892.

Quehenberger O, Prossnitz ER, Cavanagh SL, Cochrane CG and Ye RD (1993) Multiple domains of the N-formyl peptide receptor are required for high-affinity ligand binding. Construction and analysis of chimeric N-formyl peptide receptors. *J Biol Chem* **268**:18167-18175.

Rao TS, Currie JL, Shaffer AF and Isakson PC (1993) Comparative evaluation of arachidonic acid (AA)- and tetradecanoylphorbol acetate (TPA)-induced dermal inflammation. *Inflammation* **17**:723-741.

Tian Q, Li J, Xie X, Sun M, Sang H, Zhou C, An T, Hu L, Ye RD and Wang MW (2005) Stereospecific induction of nuclear factor-kappaB activation by isochamaejasmin. *Mol Pharmacol* **68**:1534-1542.

Yan P, Nanamori M, Sun M, Zhou C, Cheng N, Li N, Zheng W, Xiao L, Xie X, Ye RD and Wang MW (2006) The immunosuppressant cyclosporin A antagonizes human formyl peptide receptor through inhibition of cognate ligand binding. *J Immunol* **177**:7050-7058.

Ye RD, Cavanagh SL, Quehenberger O, Prossnitz ER and Cochrane CG (1992) Isolation of a cDNA that encodes a novel granulocyte N-formyl peptide receptor. *Biochem Biophys Res Commun* **184**:582-589.

MOL 37564

Footnotes

This project was supported in part by grants from the Ministry of Science and Technology of China (2004CB518902 to **M.-W.W.**), Chinese Academy of Sciences (KSCX1-SW-11-2 to **M.-W.W.**), Shanghai Municipality Science and Technology Development Fund (05DZ22914 and 06DZ22907 to **M.-W.W.**), and National Institutes of Health (AI033503 to **R.D.Y.**).

C.Z. and S.Z. contributed equally to this work. Reprint request or correspondence can also be addressed to Dr. Richard D. Ye, Department of Pharmacology, University of Illinois at Chicago, 835 South Wolcott Avenue, M/C 868, Chicago, IL 60612. E-mail: yer@uic.edu

MOL 37564

Legends for figures

Figure 1. The synthetic route of quinazolinone C. Reagents and conditions: a) 1. NaOH, MeOH, 0°C, 20 min 2. *n*-BuBr, MeOH, reflux, 5 h; b) N₂H₄·H₂O, MeOH, reflux, 6 h; c) 2-nitrobenzoyl chloride, Et₃N, CH₂Cl₂, 0°C to room temperature, overnight; d) Zn, AcOH, CH₂Cl₂, 0°C to room temperature, 4 h; e) substituted benzaldehyde, AcOH/DMA/CH₂Cl₂(5/5/90), 4A molecular sieve, reflux, 12 h.

Figure 2. Chemical structures of hit compound (C8) and its derivatives. A, structure of the hit compound identified from high-throughput screening and its four series derivatives (C, M, W and O). B, structures of C series derivatives at R¹. Compound C1 is the previously reported FPRL1 agonist Quin-C1. Derivatives were designed based on hit compound C8 by changing the substitution on the phenyl group at the 2-position while keeping the basic quinazolinone skeleton.

Figure 3. Identification of FPRL1, but not FPR and FPRL2, in RBL-FPRL1 and characterization of its specificity. A, gel electrophoresis data showing PCR products obtained from RBL-FPRL1-derived cDNA. Only the FPRL1 transcript was detected. The specificity of the primers used is confirmed in RT-PCR using control cDNAs for human FPR, FPRL1 and FPRL2. PCR was conducted for 30 cycles. GAPDH was used as an internal control for the quality of the RT product from RBL-FPRL1. B, calcium mobilization assay demonstrating the responsiveness of RBL-FPRL1 to C1 (100 μM), WKYMVm (W-pep), the FPRL1-selective peptide MMK1 and fMLF, a low-affinity peptide ligand for

MOL 37564

FPRL1. All peptide agonists were used at 100 nM. Representative tracings from 3 are shown.

Figure 4. Antagonist activity of compounds on WKYMVm stimulated calcium

mobilization. Different concentrations of C7 or C12 were added into RBL-FPRL1 cells 30 min before induction with 2 nM WKYMVm. The results (means \pm SEM) are expressed as relative activity compared to the maximal $[Ca^{2+}]$ release induced by 2 nM WKYMVm.

Figure 5. Effects of C7 on C1 (100 nM) or WKYMVm (10 nM) induced chemotaxis in

RBL-FPRL1 cells. Various concentrations of C7 were added before the chemotaxis assay using C1 or WKYMVm as agonists. Data (means \pm SEM) were expressed as percentage of the maximal chemotaxis and were representative of two independent experiments.

Figure 6. Competitive binding of selected C series derivatives to [125 I]WKYMVm with

FPRL1. Cell membrane was prepared from RBL-FPRL1 cells. Various concentrations of compounds were incubated together with RBL-FPRL1 cell membrane preparation, 0.16 nM [125 I]WKYMVm and FlashBlue™ GPCR beads. The plates were incubated at 4°C for 12 h and centrifuged for 3 min at $2500 \times g$ before counting on a MicroBeta scintillation counter. The results (means \pm SEM) are expressed as percent specific binding from three independent experiments.

Figure 7. Competitive binding of C7 with [3 H]fMLF. RBL-FPR cells (1×10^5) were

seeded onto 24-well plates and incubated for 48 h. After brief washing twice, cells were

MOL 37564

incubated with the blocking buffer (RPMI1640 supplemented with 25 mM HEPS and 0.1% BSA, pH7.5) for 2 h, and then treated with different concentrations of C7 or unlabeled fMLF together with 30 nM [^3H]fMLF for additional 2 h. Radioactivity was measured by a MicroBeta scintillation counter. Data (means \pm SEM) are collected from three to four independent experiments.

Figure 8. Effects of C7 on C1-induced phosphorylation of ERK. RBL-FPRL1 cells were pretreated with different concentrations of C7, or with vehicle control (DMSO of same concentration). After 15 min, the cells were stimulated with C1 (1 μM) for 5 min. Phosphorylation of ERK1 and ERK2 was determined as described in *Materials and Methods*. A representative set of blots is shown.

Figure 9. Antagonist activity of C7 on WKYMVm or C1 stimulated calcium mobilization. WRW⁴ was used as a control. Different concentrations of C7 or WRW⁴ were added into RBL-FPRL1 cells 30 min before induction with 2 nM WKYMVm (A, B) or 5 μM C1 (C, D). Data are expressed as relative activity compared to the maximal [Ca^{2+}] release induced by 2 nM WKYMVm or 5 μM C1. Results were means \pm SEM of three independent experiments.

Figure 10. Inhibition of arachidonic acid-induced ear edema by C7. BALB/c mice were treated i.p. with vehicle (1% DMSO, 19% PEG400 and 80% normal saline; Ctrl), dexamethasone (DEX, 1 mg), or various concentrations of C7 30 min before application of

MOL 37564

arachidonic acid (AA; 0.25 mg in 20 μ l of a solution containing 5% DMSO and 95% acetone). Three hours later, ear edema was determined as described in *Materials and Methods*, and expressed as ear edema rate. Data shown are means \pm SEM based on one experiment with 4-7 mice in each group.

Table 1. Bioactivities detected with the quinazolinone C derivatives.

| Compound | FPRL1 binding (IC ₅₀ , nM) ^a | Reporter assay ^b | | Calcium mobilization ^c | |
|-----------------|--|-----------------------------|--------------|-----------------------------------|--------------|
| | | EC ₅₀ (nM) | Efficacy (%) | EC ₅₀ (μM) | Efficacy (%) |
| Hit (C8) | 745±104 | 472±9 | 54.3±0.1 | 12.34±0.83 | 43±3 |
| C1 | 92±1 | 15±4 | 88.5±9.1 | 0.47±0.02 | 90±4 |
| C5 | 174±61 | 46±10 | 87.6±5.0 | 1.48±0.15 | 74±4 |
| C7 | 6653±859 | <i>n.a.</i> | <i>n.a.</i> | <i>n.a.</i> | <i>n.a.</i> |
| C9 | >15000 | 8064±487 | 52.7±4.2 | <i>n.a.</i> | <i>n.a.</i> |
| C10 | 261±59 | 89±8 | 86.7±11.5 | 1.10±0.17 | 55±3 |
| C11 | >15000 | 1352±201 | 31.1±3.9 | <i>n.a.</i> | <i>n.a.</i> |
| C12 | >15000 | <i>n.a.</i> | <i>n.a.</i> | <i>n.a.</i> | <i>n.a.</i> |
| WKYMVm | 0.4±0.1 | 1.3±0.2 | 100 | 0.0011±0.0001 | 100 |

^aThe compounds were evaluated for their binding abilities to FPRL1 in competition with [¹²⁵I]WKYMVm.

^bAgonist activities were assessed in HeLa cells stably transfected with human FPRL1 gene and a pNF-κB-Luc reporter plasmid. ^cCalcium responses were examined in RBL-2H3 cells stably transfected with human FPRL1 genes (RBL-FPRL1). Efficacy was expressed as percentage of the maximal response that elicited by 10 μM (in the reporter assay) or 1 μM (in the calcium mobilization assay) WKYMVm. *n.a.* no activity (efficacy <15%, or potency >20 μM). Each value represents means ± SEM of three independent experiments.

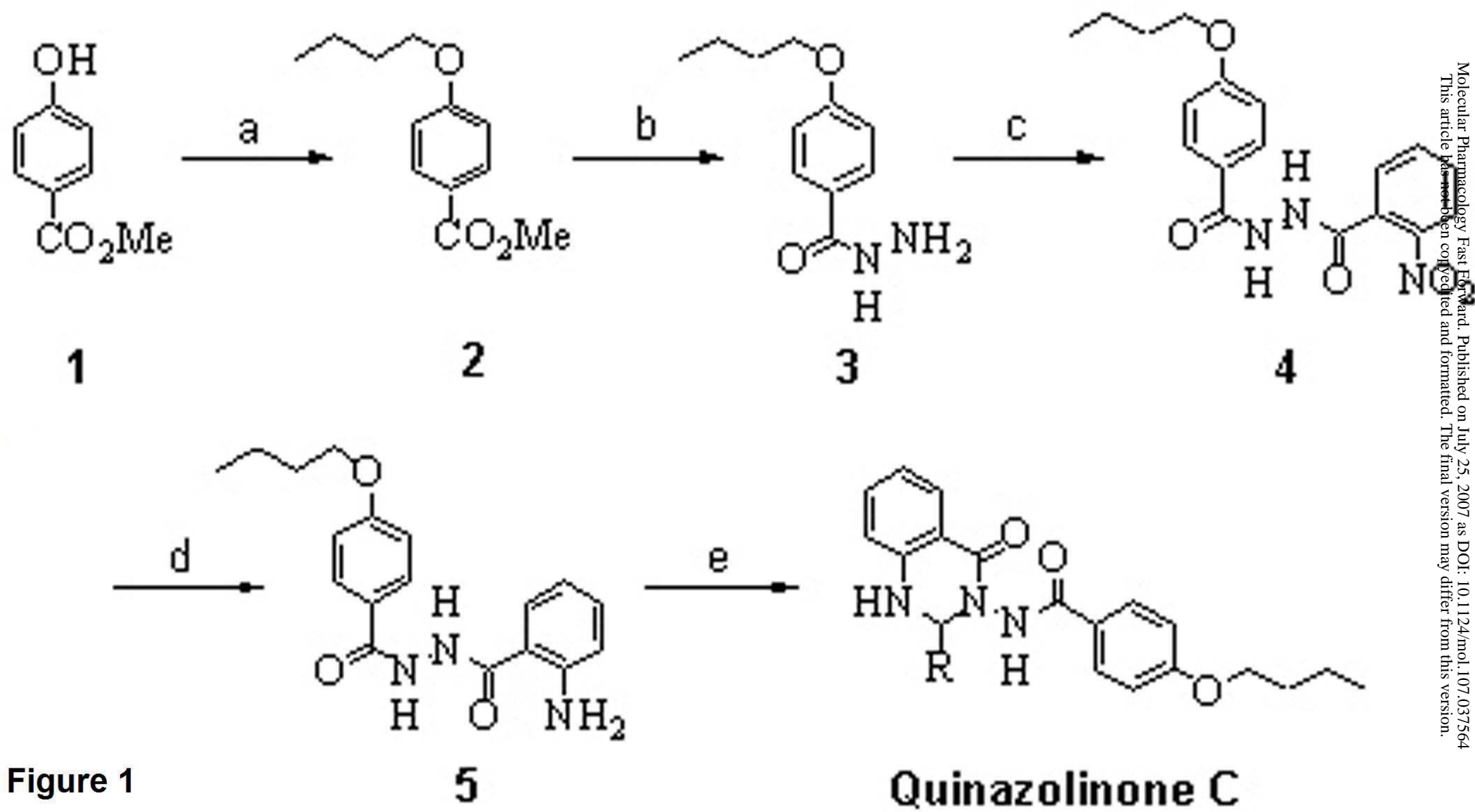
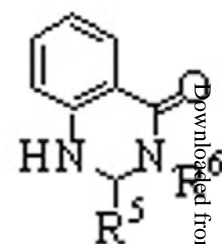
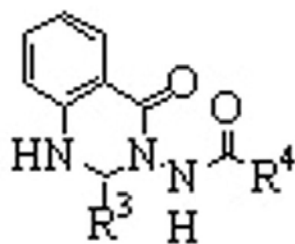
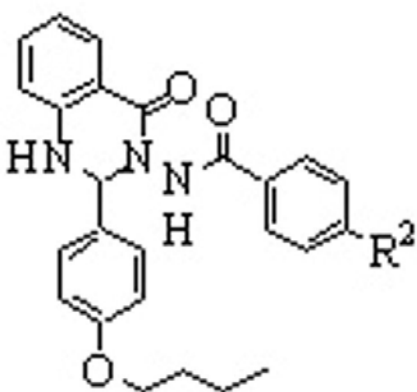
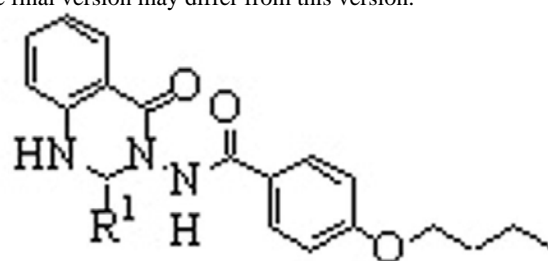
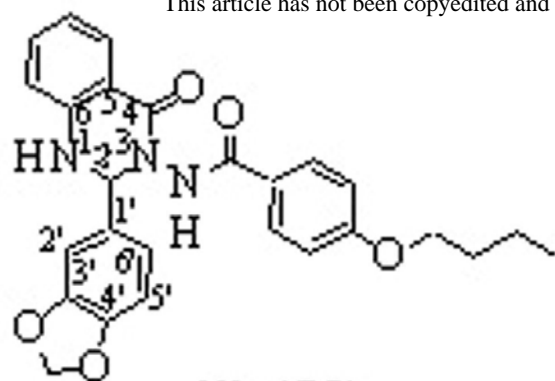


Figure 1

A



M s e r i e s

W series

0 series

B

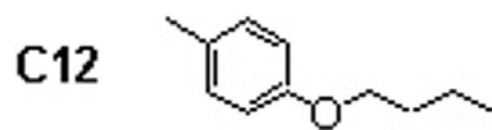
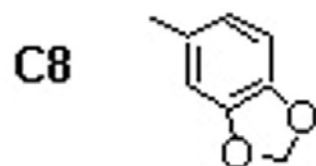
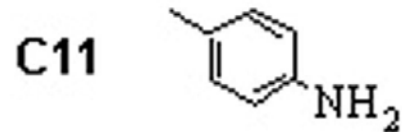
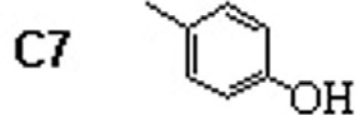
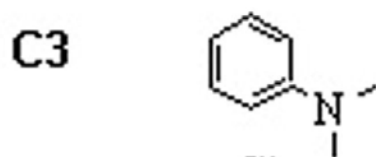
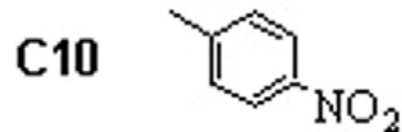
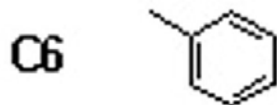
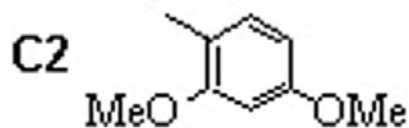
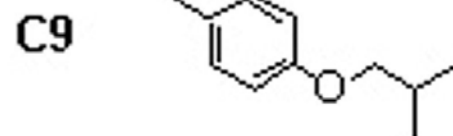
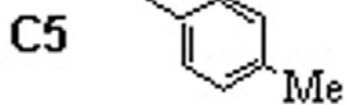
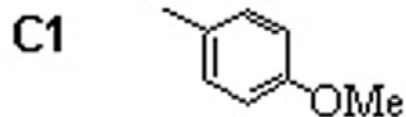
 \mathbb{R}^1 

Figure 2

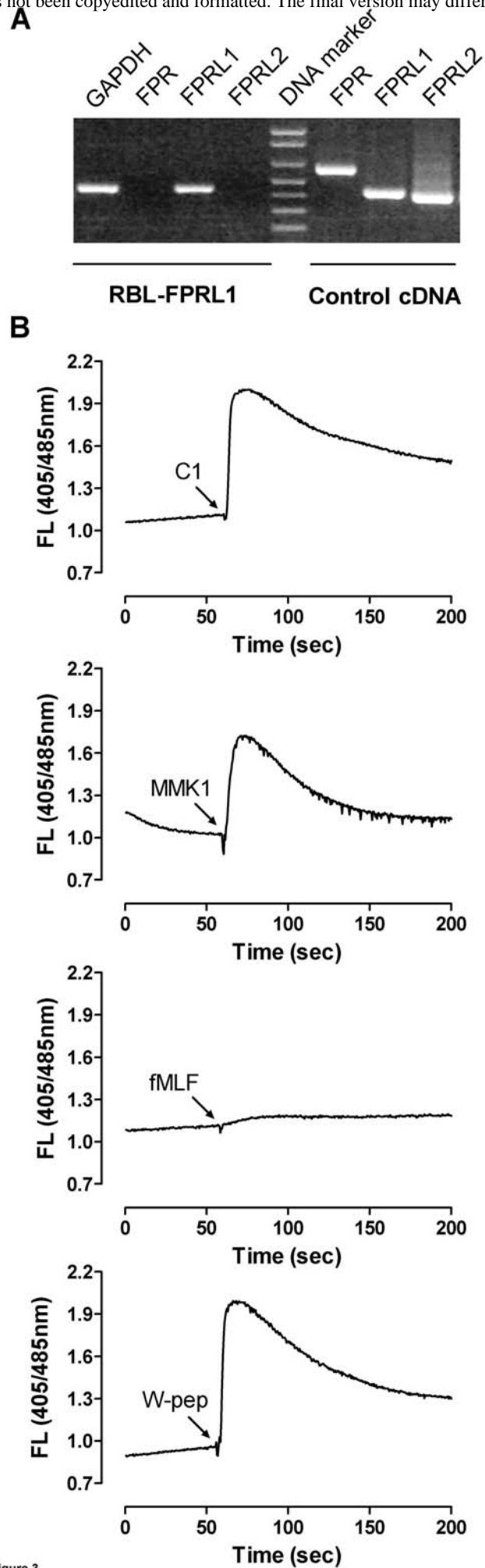


Figure 3

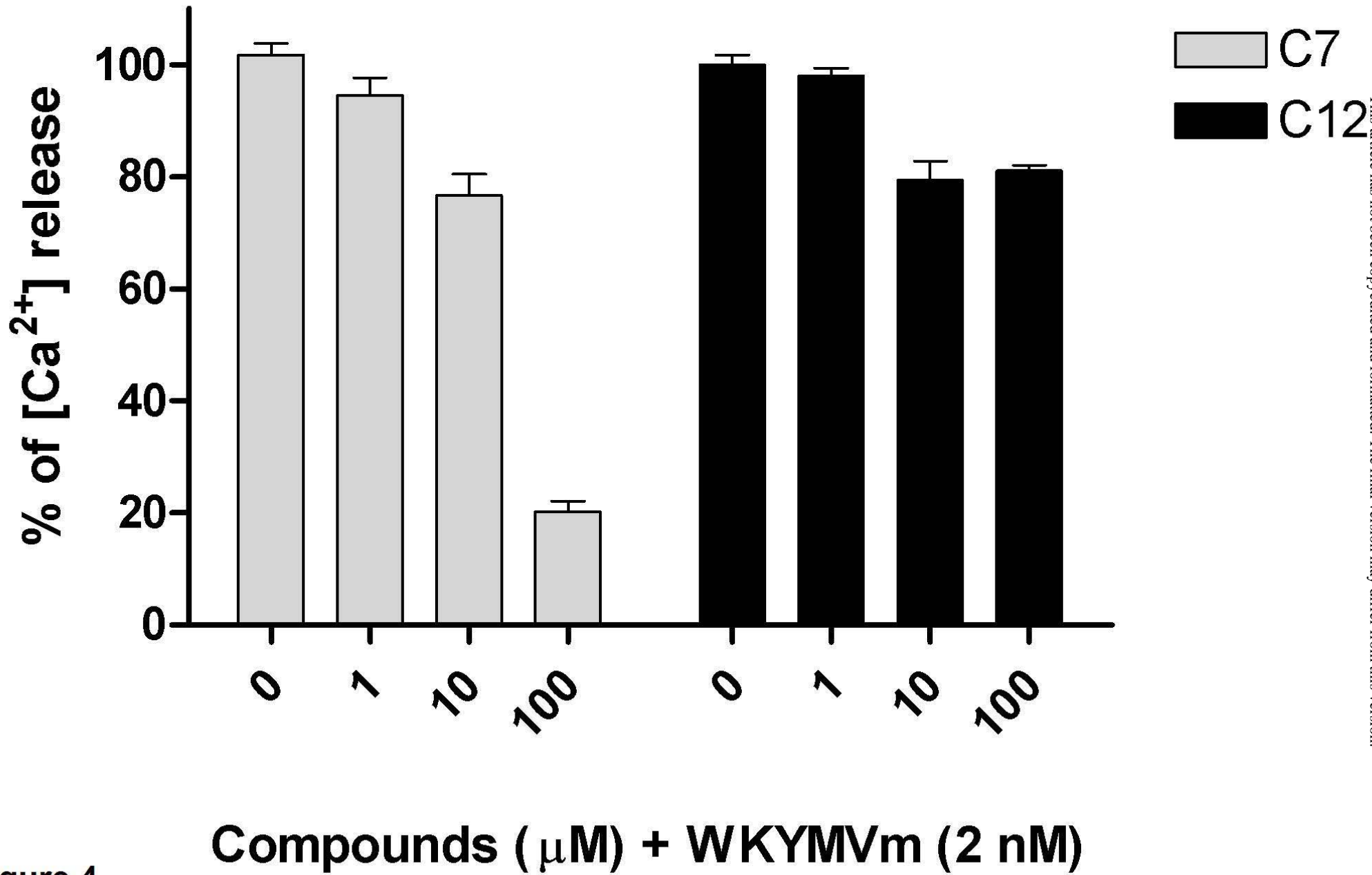


Figure 4

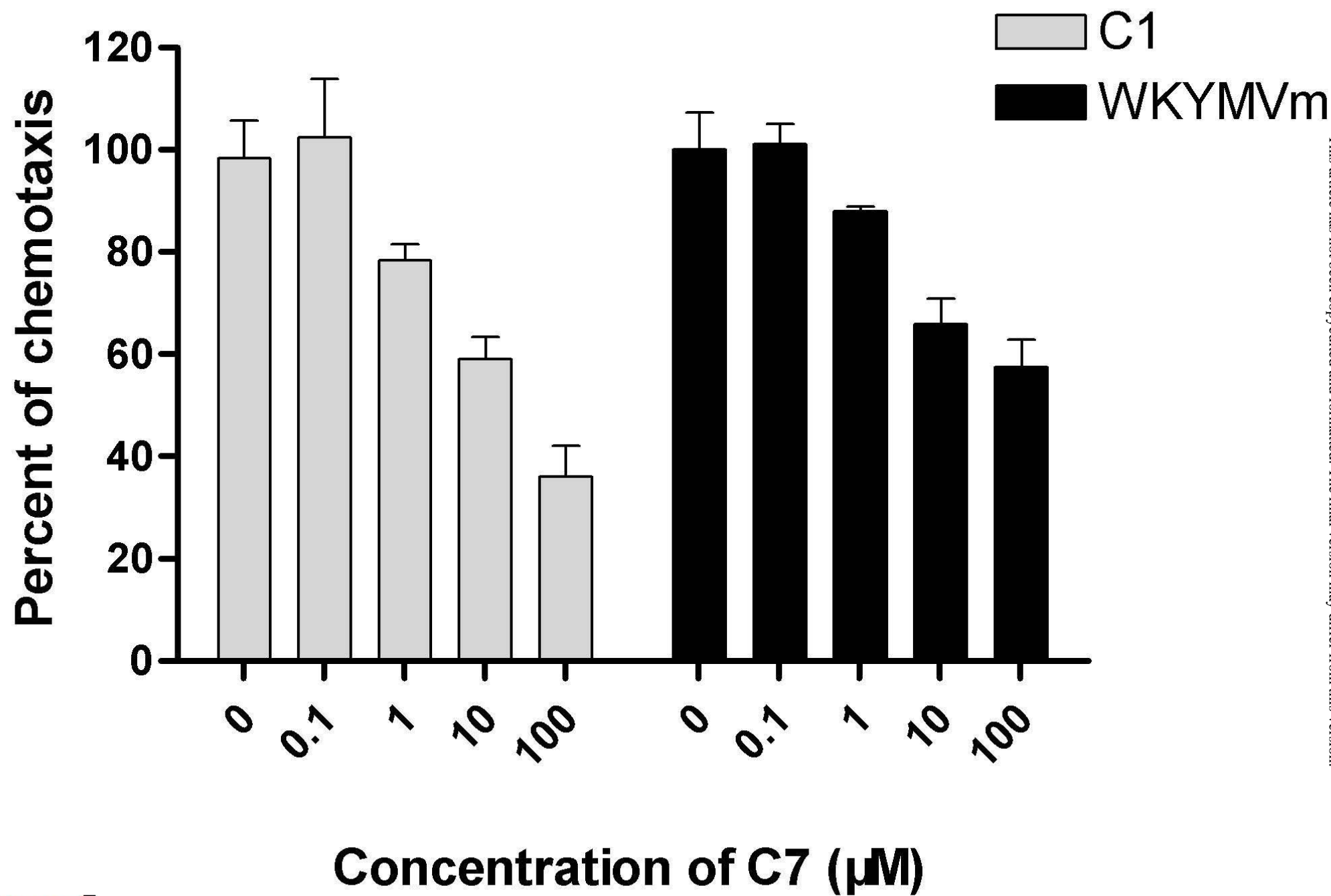


Figure 5

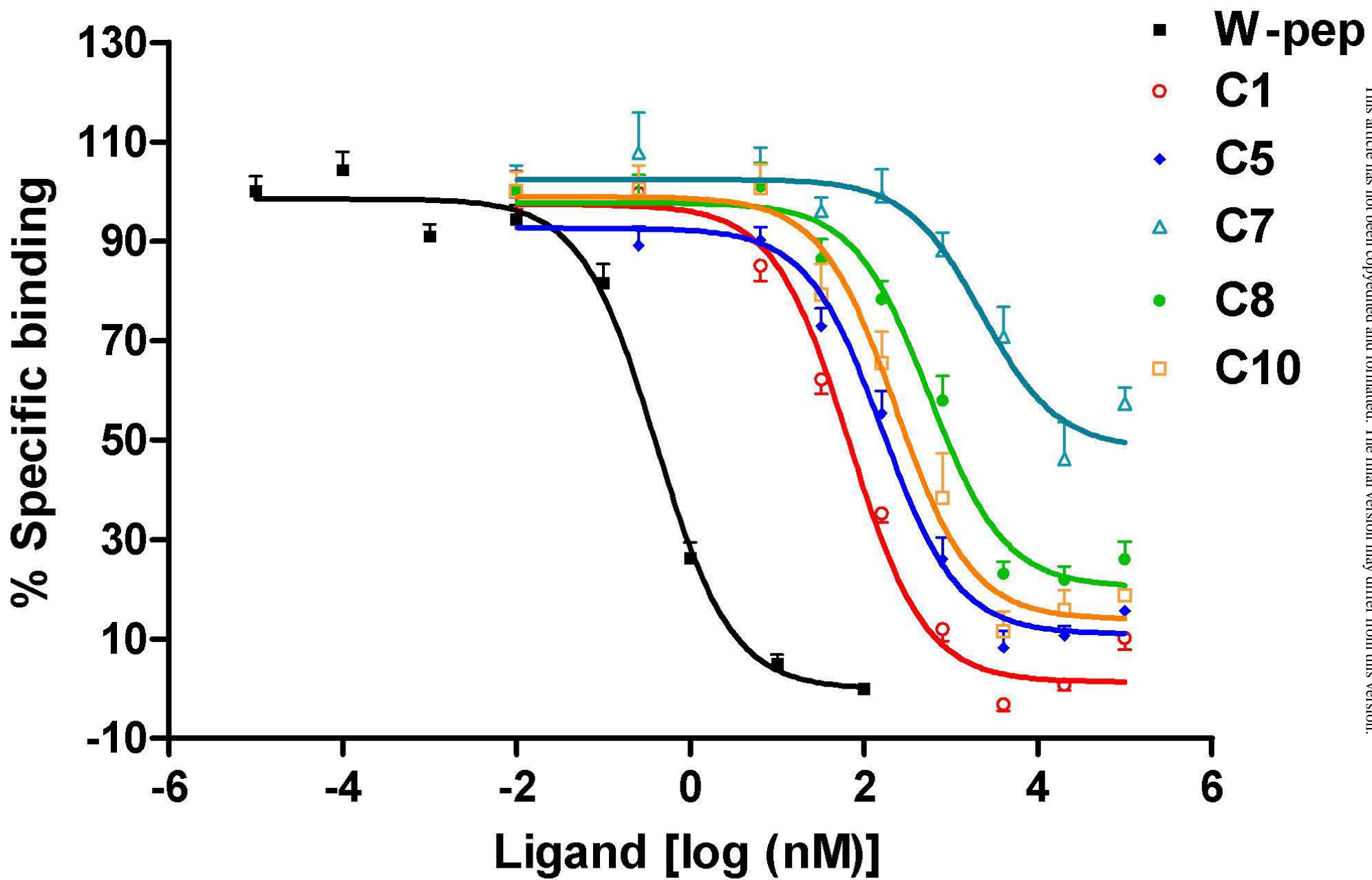


Figure 6

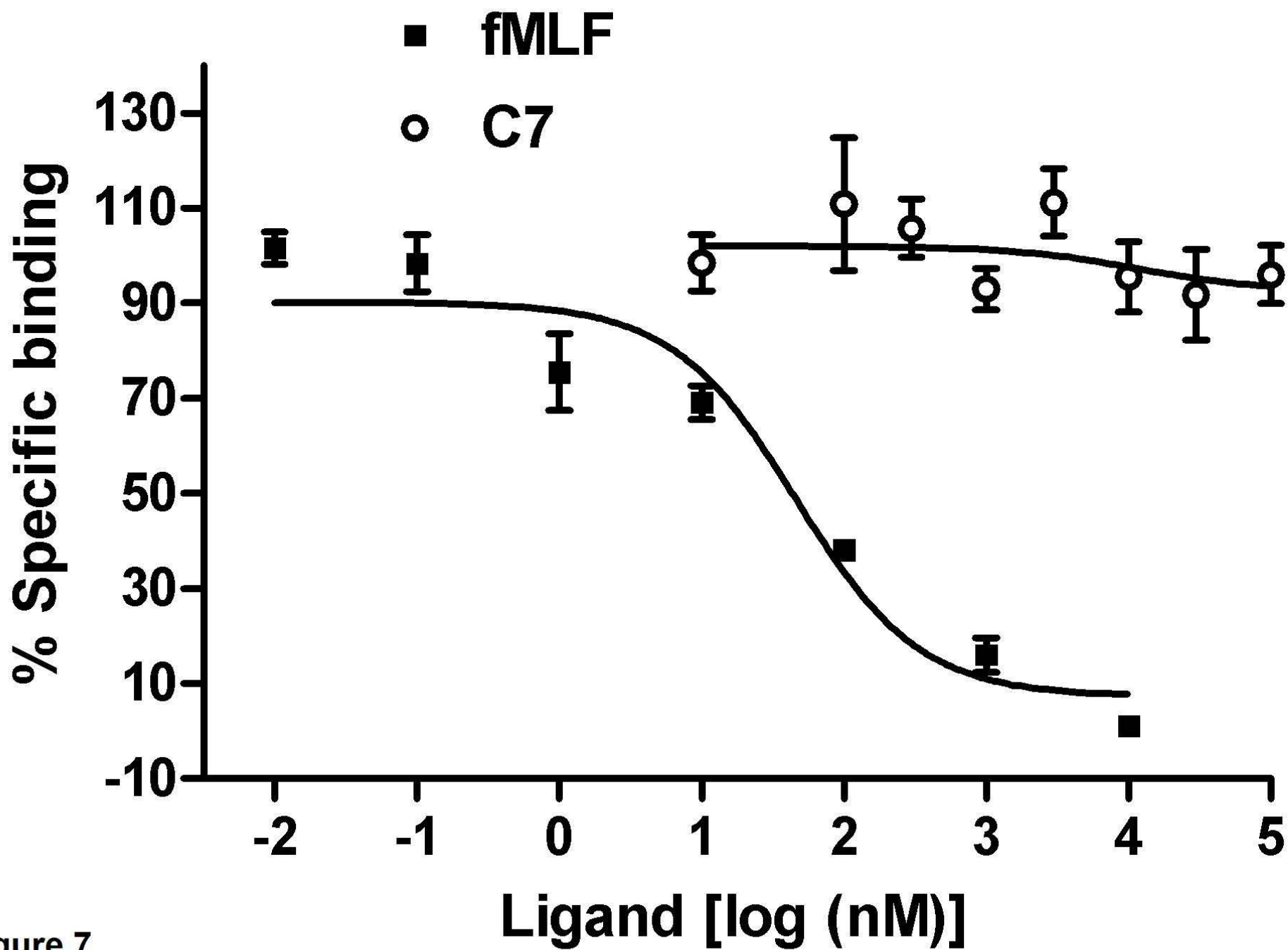
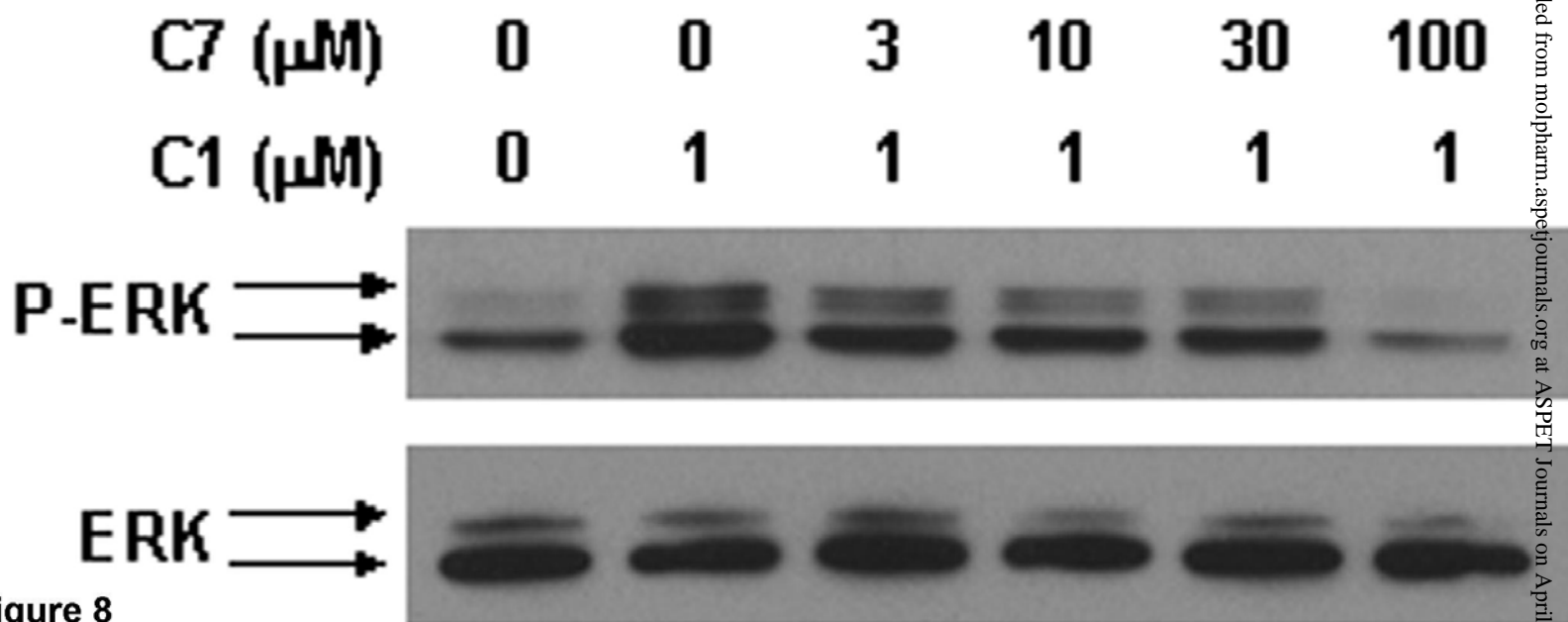


Figure 7



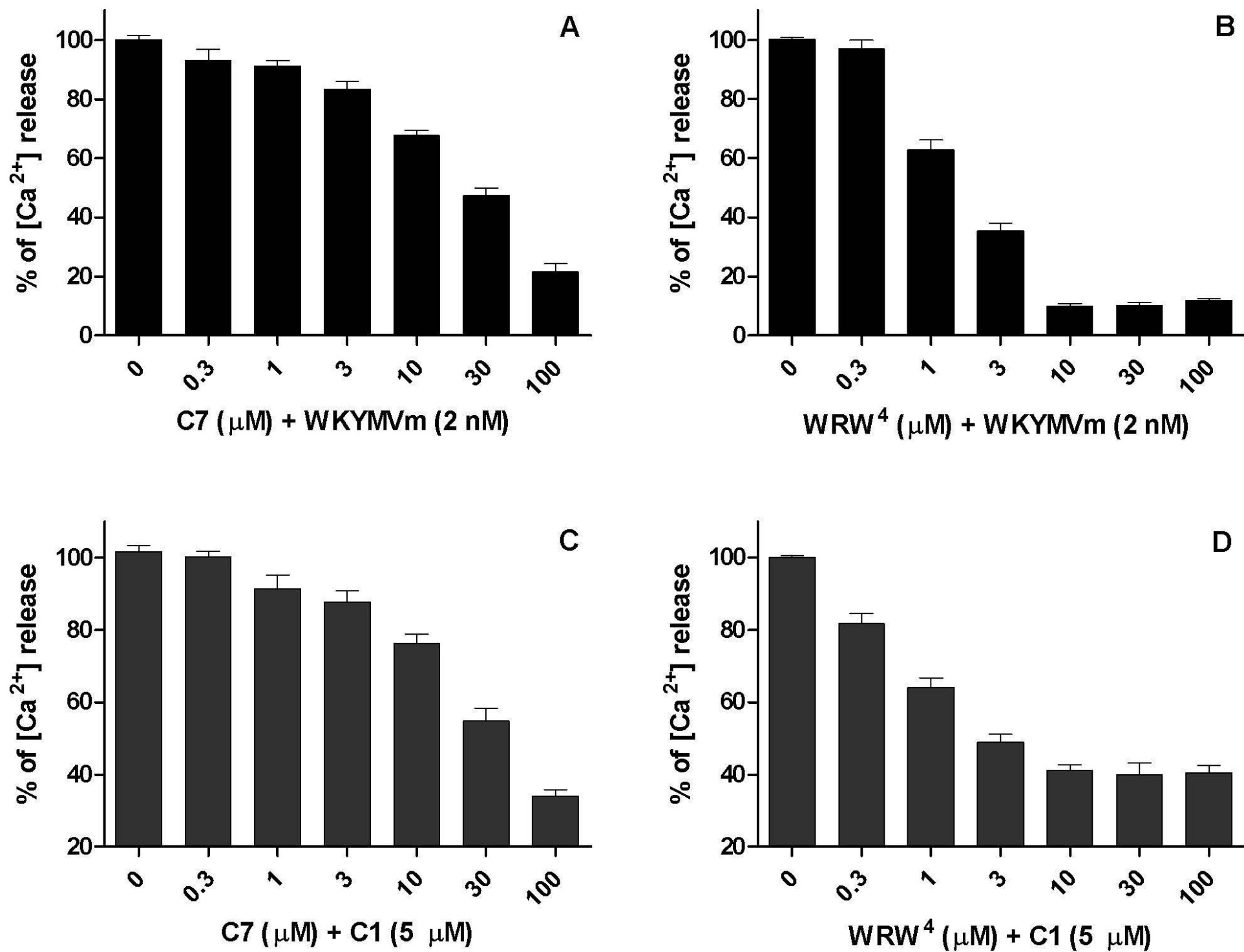


Figure 9

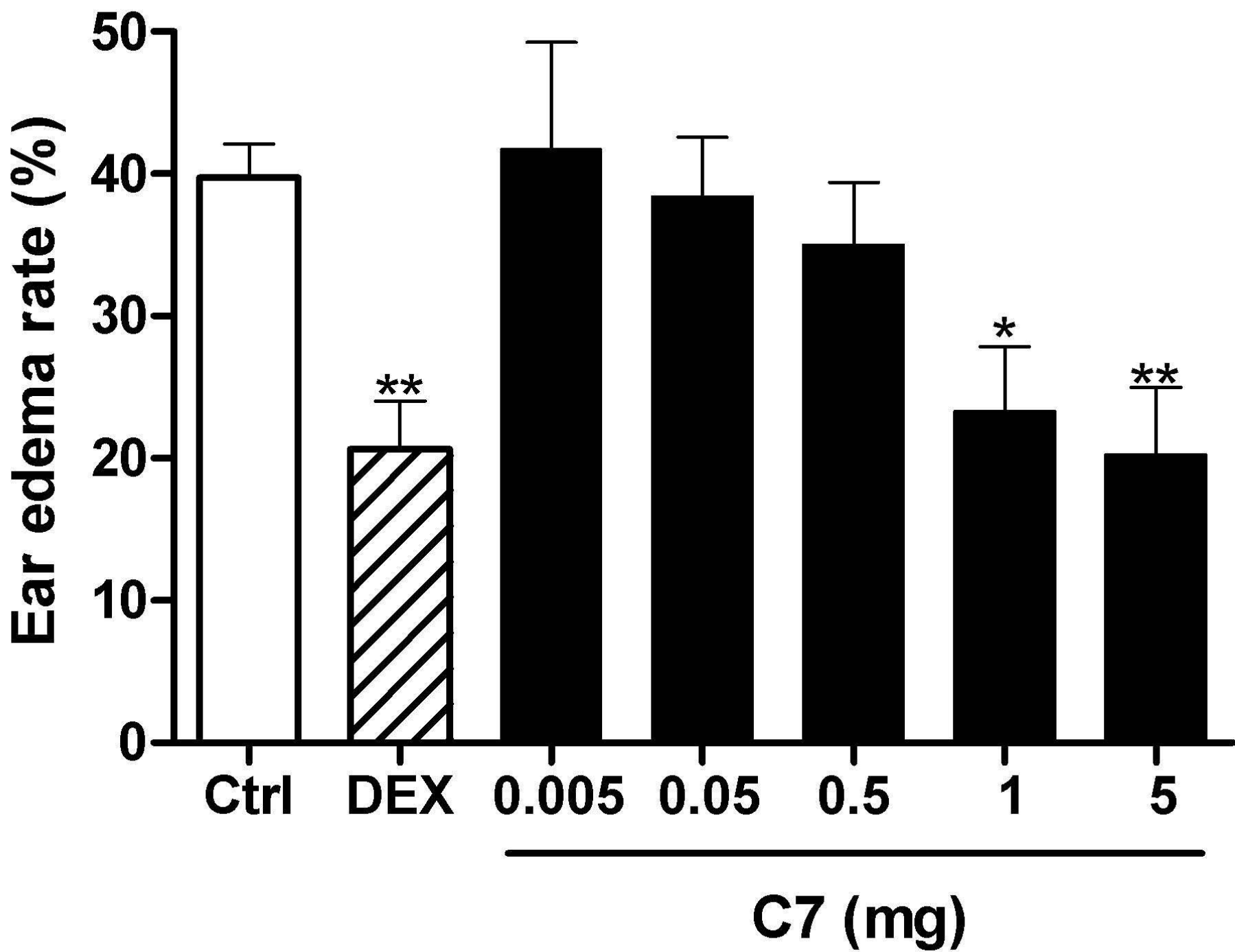


Figure 10